HNUE JOURNAL OF SCIENCE DOI: 10.18173/2354-1059.2021-0045
Natural Sciences 2021, Volume 66, Issue 3, pp. 38-51
This paper is available online at http://stdb.hnue.edu.vn

EQUILIBRIUM VACANCY CONCENTRATION AND THERMODYNAMIC QUANTITIES OF FCC DEFECTIVE ALLOYS AuCuSi AND PtCuSi UNDER PRESSURE AND TEMPERATURE

Le Hong Viet[1] and Nguyen Quang Hoc[2]

[1]*Faculty of Fundamental Sciences, Tran Quoc Tuan University*
[2]*Faculty of Physics, Hanoi National University of Education*

Abstract. We present the analytic expressions of the cohesive energy, the alloy parameters, the equation of state, the mean nearest neighbor distance, the Helmholtz free energy, equilibrium vacancy concentration, and thermodynamic quantities such as the isothermal compressibility, the thermal expansion coefficient, the heat capacities at constant volume and constant pressure for face-centered cubic (FCC) defective ternary substitutional and interstitial alloy ABC derived by the statistical moment method (SMM). The obtained thermodynamic quantities depend on temperature, pressure, the concentration of substitutional atoms, the concentration of interstitial atoms, and equilibrium vacancy concentration. Thermodynamic quantities of FCC defective metal A, FCC defective substitutional alloy AB, and FCC defective interstitial alloy AC are specific cases for thermodynamic quantities of FCC defective ternary substitutional and interstitial alloy ABC. The theoretical results are calculated numerically to alloys AuCuSi and PtCuSi. Our calculated results of thermal expansion coefficient and heat capacities at constant pressure for main metals Au, Pt are in good agreement with experimental data. Our other calculated results for thermodynamic quantities of alloys AuCuSi and PtCuSi at different temperatures, pressure, the concentration of substitutional atoms, and concentrations of interstitial atoms orient and predict new experimental data in the future.

Keywords: substitutional and interstitial alloy, equilibrium vacancy concentration, perfective alloy, defective alloy, statistical moment method.

1. Introduction

Interstitial alloys such as AuCuSi and PtCuSi are extremely important in science and technology. Gold, platinum, and their alloys are widely used in structural, electrical, and other technological applications; thus, it is vital to have accurate values of their basic physical properties. Among physical properties, the thermodynamic quantities are

---

Received August 17, 2021. Revised October 18, 2021. Accepted October 25, 2021.

Contact: Le Hong Viet, e-mail address: levietmat@gmail.com

of both fundamental and practical interests. Information on the influences of pressure and temperature on the thermodynamic properties of crystals plays an essential role in predicting and understanding the interatomic interactions, strength, mechanical stability, phase transition mechanisms, and dynamical response of materials.

Silicides such as AuSi have attracted a lot of attention in recent years because of their functional applications and unusual physical properties. Gold silicide or gold silicon is one of the numerous metal alloys sold by American Elements under the trade name AE Alloys^{TM}.

Vacancies exist throughout nature and determine the physical properties of materials. By manipulating the density and distribution of vacancies, it is possible to influence their physical properties such as band-gap, conductivity, magnetism, etc. This can generate exciting applications in the fields of water treatment, energy storage, and physical devices such as resistance-change memories. Vacancy engineering is one of the most studied and effective methods to manipulate the various properties of materials from surface stability to electrical transport and band structures [1-5]. Vacancy has important influence thermodynamic properties of metals and alloys in high temperatures. We had been studied the effect of the vacancy on thermodynamic quantities of ternary and binary interstitial alloys with FCC and body-centered cubic (BCC) structures [6-13].

In the present paper, by the SMM [14, 15] we present the thermodynamic theory of FCC ternary substitutional and interstitial alloy under pressure and calculate numerically for alloys AuCuSi and PtCuSi.

2. Content

2.1. Theoretical results

The Helmholtz free energy ψ_{ABC} of perfect FCC ternary substitutional and interstitial alloy ABC (main metal atoms A are in vertices, substitutional metal atoms B are in face centers and interstitial non-metal atoms C are in body centers of cubic unit cells) with the concentration condition $c_C << c_B << c_A$ ($c_i = \frac{N_i}{N}$ is the concentration of atoms i (i = A,B,C), N_i is the number of atoms i and N is the total number of alloy) is determined by [9, 13-15].

$$\psi_{ABC} = \psi_{AC} + c_B\left(\psi_B - \psi_A\right) + TS_c^{AC} - TS_c^{ABC}, \tag{1}$$

$$\psi_{AC} = \sum_X c_X \psi_X - TS_c^{AC} \, (X = C, A, A_1, A_2), \tag{2}$$

$$\psi_X = U_{0X} + \psi_{0X} + 3N\left\{\frac{\theta^2}{k_X^2}\left[\gamma_{2X}Y_X^2 - \frac{2\gamma_{1X}}{3}\left(1+\frac{Y_X}{2}\right)\right] + \right.$$

$$\left. + \frac{2\theta^3}{k_X^4}\left[\frac{4}{3}\gamma_{2X}^2 Y_X\left(1+\frac{Y_X}{2}\right) - 2\left(\gamma_{1X}^2 + 2\gamma_{1X}\gamma_{2X}\right)\left(1+\frac{Y_X}{2}\right)\left(1+Y_X\right)\right]\right\}, \tag{3}$$

where ψ_{AC} is the Helmholtz free energy of FCC interstitial alloy AC, ψ_X is the Helmholtz free energy of an atom X, X = A, B, C, A_1, A_2 in formulae (1)-(3), X = A, C, A_1, A_2 in formula (2), A_1 is the main metal atom A in face centers and A_2 is the main metal atom A in vertices of cubic unit cells for interstitial alloy AC, S_c^{ABC} is the configurational entropy of substitutional and interstitial alloy ABC, S_c^{AC} is the configurational entropy of interstitial alloy AC, $c_A = 1 - c_B - 15c_C, c_A = 1 - 15c_C$, $c_{A_1} = 6c_C, c_{A_2} = 8c_C$ for FCC lattice, $U_{0X} = \frac{N}{2}u_{0X}, u_{0X}$ is the cohesive energy of atom X, $\psi_{0X} = 3N\theta\left[x_X + \ln\left(1 - e^{-2x_X}\right)\right]$, $\theta = k_{\mathrm{Bo}}T, k_{\mathrm{Bo}}$ is the Boltzmann, T is the absolute temperature, $x_X = \frac{\hbar\omega_X}{2\theta} = \frac{\hbar}{2\theta}\sqrt{\frac{k_X}{m_X}}$, $\hbar = \frac{h}{2\pi}$ is the Planck constant, k_X is the harmonic parameter of alloy for an atom X, m_X is the mass of an atom X, $Y_X \equiv x_X \coth x_X, \gamma_{1X}, \gamma_{2X}$ is the anharmonic parameters of alloy. The expressions of the cohesive energy u_{0X} and alloy parameters k_X, γ_{1X}, γ_{2X} were shown in [9, 13].

The mean nearest neighbor distance a_{ABC} between two atoms A in FCC substitutional and interstitial alloy ABC at pressure P and temperature T is determined by [9, 13-15].

$$a_{ABC} = c_{AC}a_{AC}\frac{B_{TAC}}{\overline{B_T}} + c_B a_B \frac{B_{TB}}{\overline{B_T}}, \overline{B_T} = c_{AC}B_{TAC} + c_B B_{TB}, c_{AC} = c_A + c_C, \tag{4}$$

$$B_{TAC} = \frac{1}{\chi_{TAC}} = \frac{2P + \frac{a_{AC}^2}{v_{AC}}\frac{1}{3N}\left(\frac{\partial^2\psi_{AC}}{\partial a_{AC}^2}\right)_T}{3\left(\frac{a_{AC}}{a_{0AC}}\right)^3}, B_{TB} = \frac{1}{\chi_{TB}} = \frac{2P + \frac{a_B^2}{v_B}\frac{1}{3N}\left(\frac{\partial^2\psi_B}{\partial a_B^2}\right)_T}{3\left(\frac{a_B}{a_{0B}}\right)^3}, \tag{5}$$

$$\left(\frac{\partial^2\psi_{AC}}{\partial a_{AC}^2}\right)_T \approx \sum_X c_X\left(\frac{\partial^2\psi_X}{\partial a_X^2}\right)_T \left(X = C, A, A_1, A_2\right), \tag{6}$$

$$\frac{1}{3N}\left(\frac{\partial^2\psi_X}{\partial a_X^2}\right)_T = \frac{1}{6}\frac{\partial^2 u_{0X}}{\partial a_X^2} + \frac{\hbar\omega_X}{4k_X}\left[\frac{\partial^2 k_X}{\partial a_X^2} - \frac{1}{2k_X}\left(\frac{\partial k_X}{\partial a_X}\right)^2\right], \tag{7}$$

where a_{AC} is the mean nearest neighbor distance between two atoms A in FCC interstitial alloy AC, a_B is the nearest neighbor distance between two atoms in FCC metal B, B_{TAC}, χ_{TAC} are the isothermal elastic modulus and the isothermal compressibility of alloy AC, B_{TB}, χ_{TB} the isothermal elastic modulus and the isothermal compressibility of metal B, $\overline{B_T}$ is the mean isothermal compressibility of alloy ABC and P is the pressure.

The nearest neighbor distance a_X between two atoms X in material X at pressure *P* and temperature *T* is derived from the equation of state for material X [9, 13-15].

$$Pv_X = -a_X\left(\frac{1}{6}\frac{\partial u_{0X}}{\partial a_X} + \frac{\theta Y_X}{k_X}\frac{\partial k_X}{\partial a_X}\right), v_X = \frac{\sqrt{2}a_X^3}{2}. \tag{8}$$

The Helmholtz free energy ψ^R_{ABC} of defective FCC ternary substitutional and interstitial alloy ABC has the form [9, 13].

$$\psi^R_{ABC} = \sum_X \left\{\left[1 - n_v n_1 + n_v\left(B_X - 1\right)\right]c_X\psi_X + n_v n_1 c_X \psi_X^{(1)}\right\} - T\left(S_c^{ABC*} + S_c^{ABC}\right), \tag{9}$$

where n_v is the equilibrium vacancy concentration, n_1 is the number of atoms on the first coordination sphere, $B_X \approx 1 + \frac{U_{0X}}{\psi_X}$, $\psi_X^{(1)}$ is the Helmholtz free energy of an atom X on the first coordination sphere with the sphere centre at the position of vacancy and S_c^{ABC*} is the configurational entropy of defective alloy ABC.

The equilibrium vacancy concentration n_v of defective FCC alloy ABC is given by [9, 13].

$$n_v^{ABC} = n_v^A \exp\left(-\frac{c_B g_v^f(B)}{\theta}\right)\exp\left(-\frac{c_C g_v^f(C)}{\theta}\right), n_v^A = \exp\left(-\frac{\sum\limits_X c_X g_v^f(X)}{\theta}\right), \left(X = A, A_1, A_2\right). \tag{10}$$

$$g_v^f\left(X\right) = n_1\left(\psi_{XX}^{(1)} - \psi_{XX}\right) + \left(B_X - 1\right)\psi_{XX}, N\psi_{XX}^{(1)} = \psi_X^{(1)}, N\psi_{XX} = \psi_X, \tag{11}$$

where $g_v^f(ABC) = \sum\limits_X g_v^f(X)$ is the change of the Gibbs thermodynamic potential of defective alloy ABC in order to form a vacancy and $g_v^f(X)$ is the change of the Gibbs thermodynamic potential of an atom X in order to form a vacancy.

The isothermal elastic modulus and the isothermal compressibility of defective alloy ABC are equal to [9, 13].

$$\chi^R_{TABC} = \frac{3\left(\frac{a_{ABC}}{a_{0ABC}}\right)^3}{2P + \frac{a_{ABC}^2}{v_{ABC}}\frac{1}{3N}\left(\frac{\partial^2\psi^R_{ABC}}{\partial a_{ABC}^2}\right)_T}, B^R_{TABC} = \frac{1}{\chi^R_{TABC}}, \tag{12}$$

$$\left(\frac{\partial^2\psi^R_{ABC}}{\partial a_{ABC}^2}\right)_T \approx \sum_X \left\{\left[1 - n_v n_1 + n_v\left(B_X - 1\right)\right]c_X\left(\frac{\partial^2\psi_X}{\partial a_X^2}\right)_T + n_v n_1 c_X\left(\frac{\partial^2\psi_X^{(1)}}{\partial a_X^{(1)2}}\right)_T\right\},. \tag{13}$$

where $a_X^{(1)}$ is the nearest neighbor distance between two atoms X on the first coordination sphere with the sphere center at the position of vacancy.

The thermal expansion coefficient of defective alloy ABC has the form [9, 13].

$$\alpha_{TABC}^{R}=\sum_{X}\left\{\left[1-n_v n_1+n_v\left(B_X-1\right)\right]c_X\alpha_{TX}+n_v n_1 c_X\alpha_{TX}^{(1)}\right\},\tag{14}$$

$$\alpha_{TX}=\frac{y_X}{a_{0X}T}\left(1+\frac{\theta}{2}\frac{a'_X}{a_X}\right),a'_X=\frac{da_X}{d\theta},\alpha_{TX}^{(1)}=\frac{y_X^{(1)}}{a_{0X}^{(1)}T}\left(1+\frac{\theta}{2}\frac{a_X'^{(1)}}{a_X^{(1)}}\right),a_X'^{(1)}=\frac{da_X^{(1)}}{d\theta},\tag{15}$$

where $a_{0X}^{(1)}$ is the nearest neighbor distance between two atoms X at T = 0K on the first coordination sphere with the sphere center at the position of vacancy, α_{TX} is the thermal expansion coefficient of an atom X and $\alpha_{TX}^{(1)}$ is the thermal expansion coefficient of an atom X on the first coordination sphere with the sphere center at the position of vacancy.

The heat capacity at constant volume of defective alloy ABC is given by [9, 13].

$$C_{VABC}^{R}=\sum_{X}\left\{\left[1-n_v n_1+n_v\left(B_X-1\right)\right]c_X C_{VX}+n_v n_1 c_X C_{VX}^{(1)}\right\},\tag{16}$$

where C_{VX} is the heat capacity at the constant volume of an atom X and $C_{VX}^{(1)}$ is is the heat capacity at constant volume on the first coordination sphere with the sphere center at the position of vacancy.

The heat capacity at a constant pressure of defective alloy ABC is determined by [9, 13].

$$C_{PABC}^{R}=C_{VABC}^{R}+\frac{9TV_{ABC}\alpha_{TABC}^{R2}}{\chi_{TABC}^{R}}.\tag{17}$$

2.2. Numerical results and discussions for alloy AuCuSi and PtCuSi

To describe the interactions Au-Au, Cu-Cu, Pt-Pt, and Si-Si in alloys AuCuSi and tCuSi, we apply the Mie-Lennard-Jones pair interaction potential in the form [16].

$$\varphi(r)=\frac{D}{n-m}\left[m\left(\frac{r_0}{r}\right)^n-n\left(\frac{r_0}{r}\right)^m\right],\tag{18}$$

where D is the depth of potential well corresponding to the equilibrium distance r_0, m and n are determined empirically. Then, the potential parameters for the interactions Au-Si, Au-Cu, Pt-Si, Pt-Cu are approximately determined by

$$\varphi_{\text{Au-Si}}\approx\frac{1}{2}\left(\varphi_{\text{Au-Au}}+\varphi_{\text{Si-Si}}\right),\varphi_{\text{Au-Cu}}\approx\frac{1}{2}\left(\varphi_{\text{Au-Au}}+\varphi_{\text{Cu-Cu}}\right),$$

$$\varphi_{\text{Pt-Si}}\approx\frac{1}{2}\left(\varphi_{\text{Pt-Pt}}+\varphi_{\text{Si-Si}}\right),\varphi_{\text{Pt-Cu}}\approx\frac{1}{2}\left(\varphi_{\text{Pt-Pt}}+\varphi_{\text{Cu-Cu}}\right).\tag{19}$$

We neglected the interactions Cu-Pt in these alloys. The Mie-Lennard-Jones potential parameters for the interactions Au-Au, Cu-Cu, Pt-Pt, and Si-Si are given in Table 1 [16].

Our obtained results are illustrated in figures from Figure 1 to Figure 23. For AuCuSi in the pressure range from zero to 12 GPa and the temperature range from 800 to 1300K, the equilibrium vacancy concentrations n_v are in the range from 10^{-5} to 10^{-3}. This result is in good agreement with experiments for Au at high pressures and temperatures.

Table 1. The Mie-Lennard-Jones potential parameters for interactions Au-Au, Cu-Cu, Pt-Pt and Si-Si

Interaction	***m***	***n***	***D***$(10^{-16}$ **erg)**	r_0**(10-^{10}m)**
Cu-Cu	5.5	11	6469.518	2.5487
Au-Au	5.5	10.5	4683	2.8751
Pt-Pt	5	9.2	9914.196	2.7689
Si-Si	6	12	45128.34	2.295

n_v strongly depends on temperature and pressure. When temperature and pressure increase, n_v also increases. Near the melting point of Au, n_v strongly increases. In low temperature and pressure, n_v is very small and then, the alloy is considered as a perfect alloy. In high temperature and pressure, n_v is significant and the influence of vacancy cannot be ignored. n_v also changes marketly according to the concentration of silicon interstitial atoms c_{Si}. When c_{Si} increases, n_v strongly decrease. For example, for AuCuSi at $c_{\text{Cu}} = 10\%$, $T = 1300$ K, $P = 8$ GPa when $c_{\text{Si}} = 0$, $n_v = 2.6867\times10^{-3}$ and when $c_{\text{Si}} = 1\%$, $n_v = 1.5794\times10^{-3}$. Then, when c_{Si} only increases 1%, n_v decreases 41%. It can be explained because when c_{Si} increases, the lattice is more tightly packed and the atoms are more difficult to move to form a vacancy. Consider the influence of the concentration of copper substitutional atoms c_{Cu} on n_v. Although c_{Cu} is much larger than c_{Si} but c_{Cu} does not significantly change n_v and other properties of the alloy. In Figure 2 and Figure 4, n_v's graphs are much closer together than n_v's graphs on Figure 1 and Figure 3. n_v increases with c_{Cu}. Due to fluctuations, the atom at the lattice can shift to form a vacancy. When tha Au atom in the crystal lattice is replaced by a Cu atom, the graph of the cohesive energy changes.

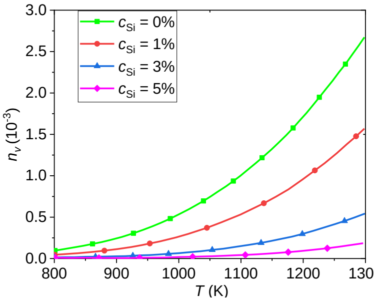

Figure 1. $n_v(T, c_{Si})$ for AuCuSi at $P = 8$ GPa, $c_{\text{Cu}} = 10\%$

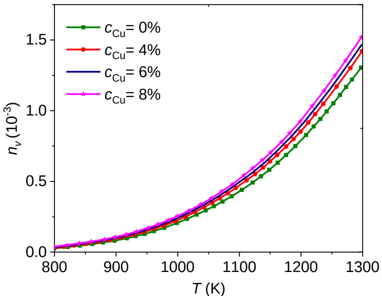

Figure 2. $n_v(T, c_{Cu})$ for AuCuSi at $P = 8$ GPa, $c_{\text{Si}} = 1\%$

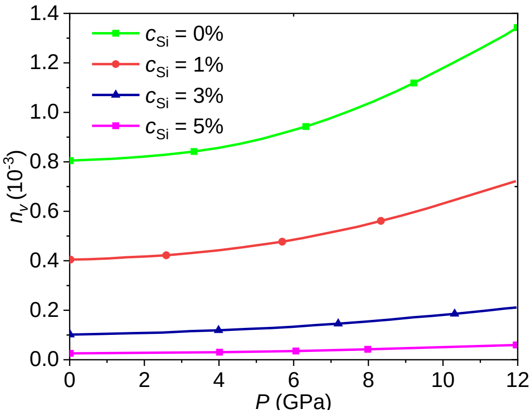

Figure 3. $n_v(P, c_{Si})$ ***for AuCuSi at T = 1100 K,*** $c_{Cu} = 10\%$

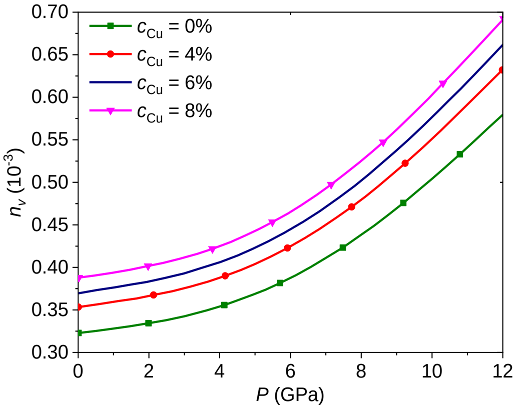

Figure 4. $n_v(P, c_{Cu})$ ***for AuCuSi at T = 1000 K,*** $c_{Si} = 1\%$

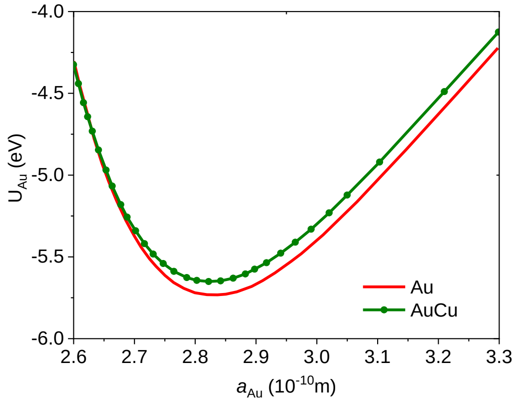

Figure 5. $u_o(a)$ ***for Au and AuCu***

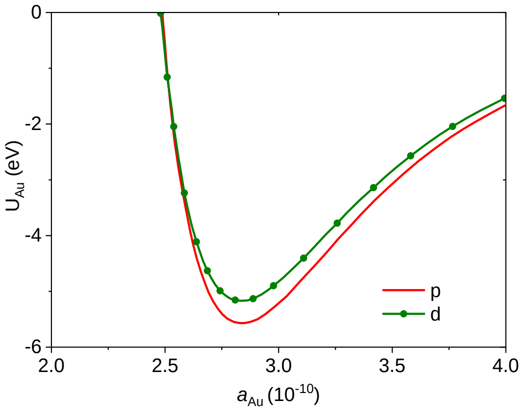

Figure 6. $u_o(a)$ ***for Au (p) and Au (d)***
(p: perfect, d: defective)

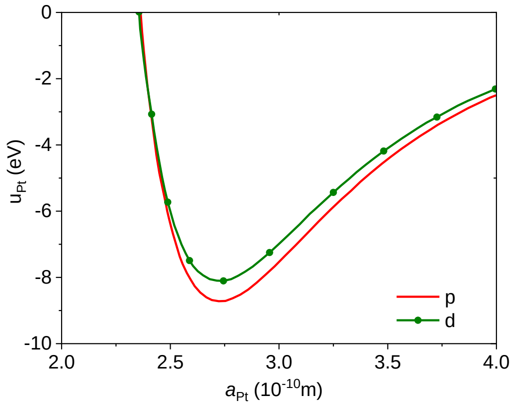

Figure 7. $u_o(a)$ ***for Pt (p) and Pt (d)***

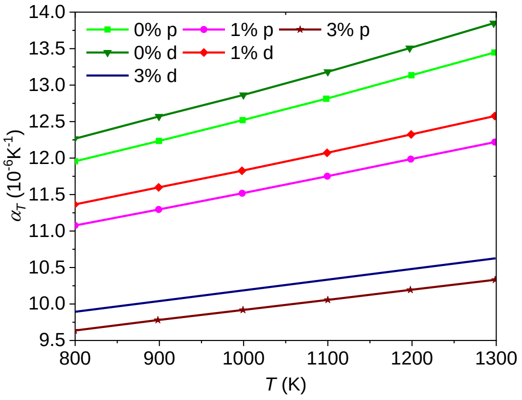

Figure 8. $\alpha_T(T, c_{Si})$ ***for AuCuSi (p) and AuCuSi (d) at P = 12 GPa,*** $c_{Cu} = 10\%$

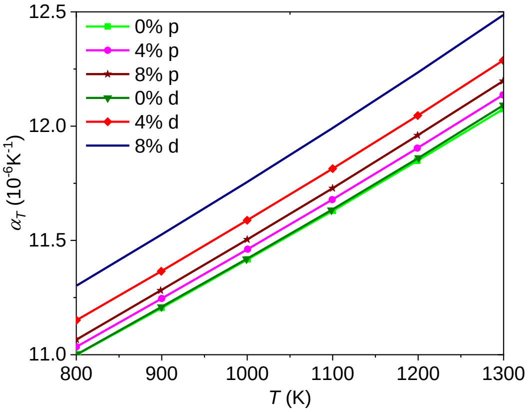

Figure 9. ***$\alpha_T(T, c_{Cu})$ for AuCuSi (p) and AuCuSi (d) at $P = 12$ GPa, $c_{Si} = 1\%$***

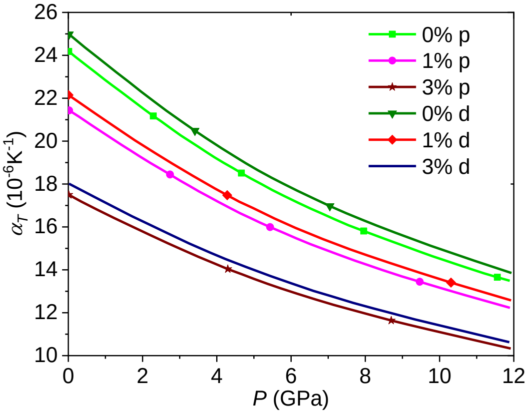

Figure 10. ***$\alpha_T(P, c_{Si})$ for AuCuSi (p) and AuCuSi (d) at $T = 1300$ K, $c_{Cu} = 10\%$***

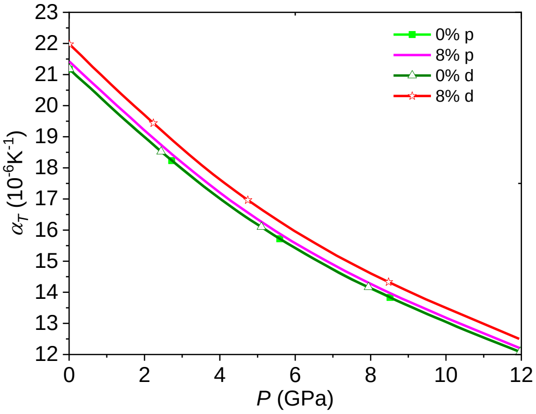

Figure 11. ***$\alpha_T(P, c_{Cu})$ for AuCuSi (p) and AuCuSi (d) at $T = 1300$ K, $c_{Si} = 1\%$***

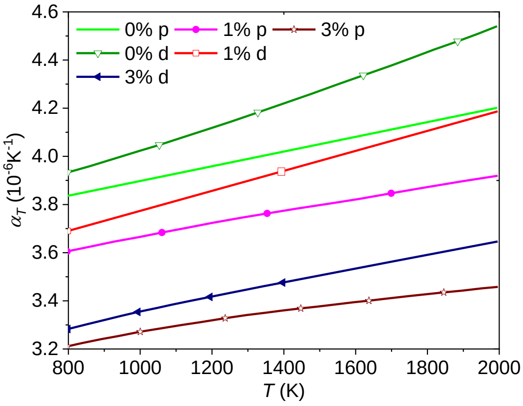

Figure 12. ***$\alpha_T(T, c_{Si})$ for AuCuSi (p) and AuCuSi (d) at $P = 80$ GPa, $c_{Cu} = 10\%$***

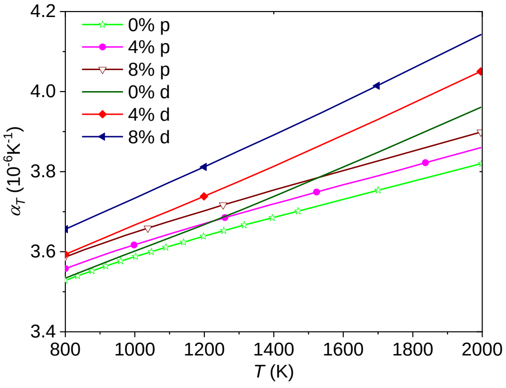

Figure 13. ***$\alpha_T(T, c_{Cu})$ for AuCuSi (p) and AuCuSi (d) at $P = 80$ GPa, $c_{Si} = 1\%$***

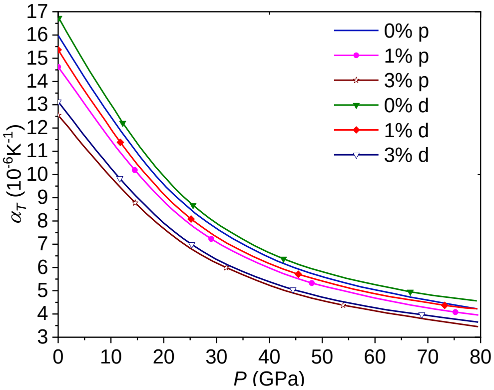

Figure 14. ***$\alpha_T(P, c_{Si})$ for AuCuSi (p) and AuCuSi (d) at $T = 2000$ K, $c_{Cu} = 10\%$***

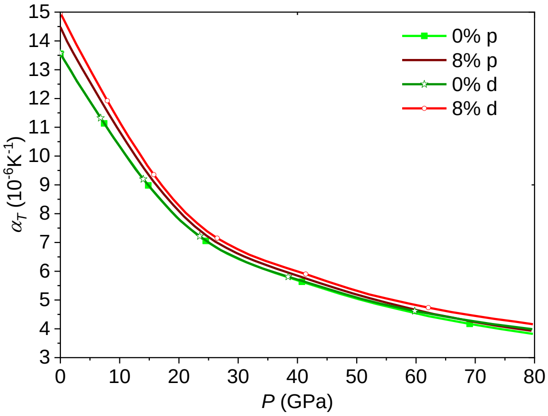

Figure 15. $\alpha_T(P, c_{Cu})$ for AuCuSi (p) and AuCuSi (d) at T = 2000 K, c_{Si} = 1%

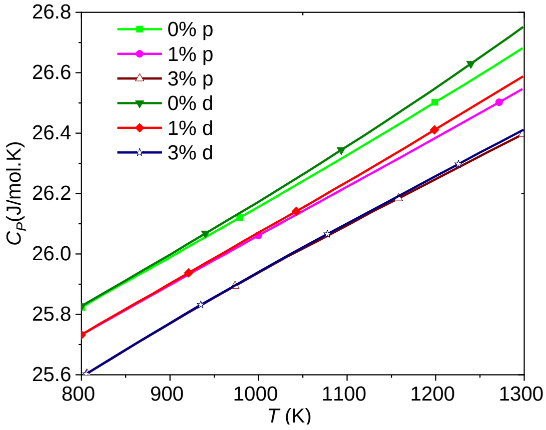

Figure 16. $C_P(T, c_{Si})$ for AuCuSi (p) and AuCuSi (d) at P = 12 GPa, c_{Cu} = 10%

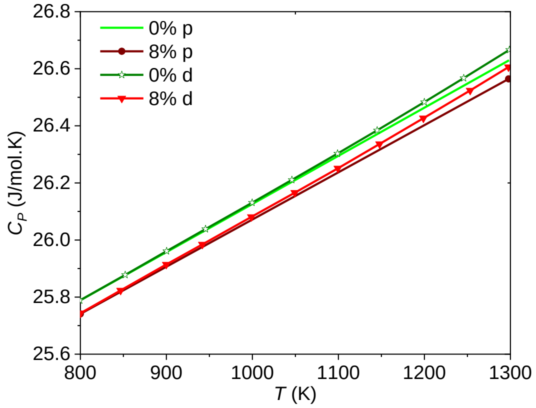

Figure 17. $C_P(T, c_{Cu})$ for AuCuSi (p) and AuCuSi (d) at P = 12 GPa, c_{Si} = 1%

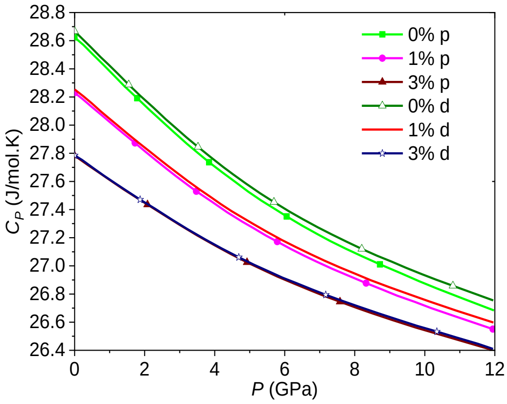

Figure 18. $C_P(P, c_{Si})$ for AuCuSi (p) and AuCuSi (d) at T = 1300 K, c_{Cu} = 10%

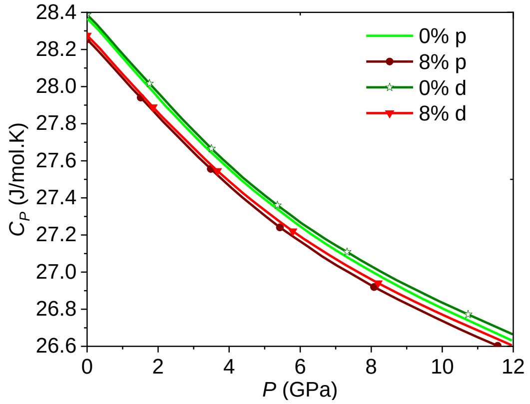

Figure 19. $C_P(P, c_{Cu})$ for AuCuSi (p) and AuCuSi (d) at T = 1300 K, c_{Si} = 1%

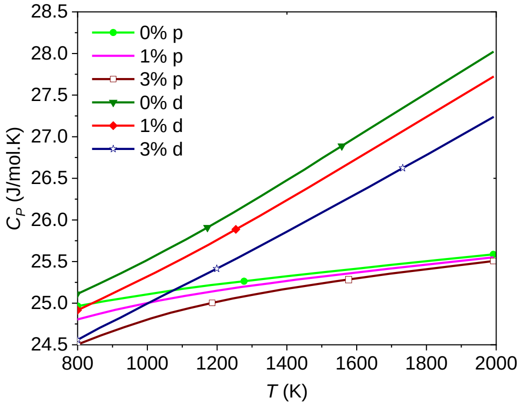

Figure 20. $C_P(T, c_{Si})$ for PtCuSi (p) and PtCuSi (d) at P = 80 GPa, c_{Cu} = 10%

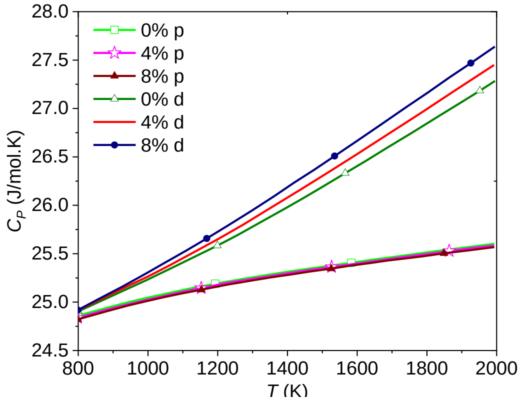

Figure 21. $C_P(T, c_{Cu})$ for PtCuSi(p) and PtCuSi (d) at P = 80 GPa, c_{Si} = 1%

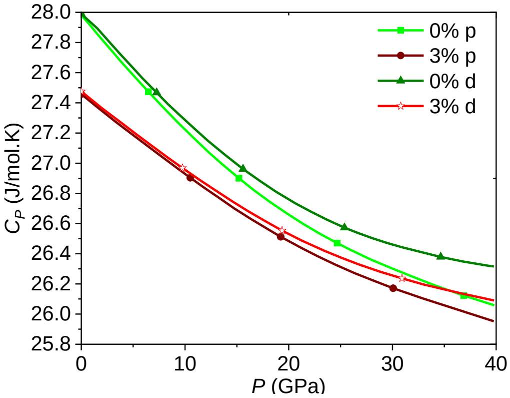

Figure 22. $C_P(P, c_{Si})$ for PtCuSi (p) and PtCuSi (d) at T = 2000 K, c_{Cu} = 10%

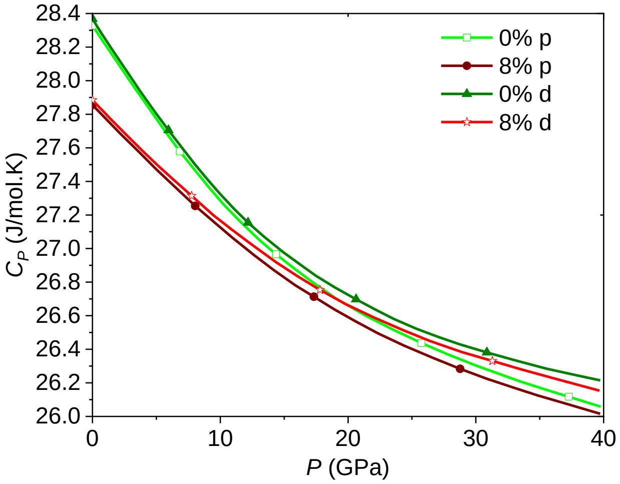

Figure 23. $C_P(P, c_{Cu})$ for PtCuSi (p) and PtCuSi (d) at T = 2000 K, c_{Si} = 1%

When the potential well is shallower, the atoms bound to the lattice are weaker and it facilitates the formation of a vacancy. The above results for n_v of AuCuSi are also true for n_v of PtCuSi. At the same temperature, pressure, and doping atomic concentration, n_v of PtCuSi is lower than n_v of AuCuSi. For example, at T = 1200 K, P = 0, c_{Cu} = 8%, c_{Si} = 1%, $n_v = 0.7131\times10^{-3}$ for AuCuSi and is 15 times larger than $n_v = 0.4603\times10^{-4}$ for PtCuSi. To get $n_v \approx 0.7\times10^{-3}$ for c_{Cu} = 8%, c_{Si} = 1%, it is possible to keep P = 0 and increase T of PtCuSi up to 1700 K or keep T = 1200 K and increase P up to 43 GPa, that is, at extremely high T and P, the vacancy has a significant effect on the properties of PtCuSi. This is because the cohesive energy u_0 in PtCuSi is much larger than the cohesive energy u_0 in AuCuSi. At P = 0, the melting temperatures of Pt and Au respectively are 2057 K and 1337 K (1.5 times less). The properties of PtCuSi in the very wide T and P up to 2000 K and 80 GPa can be considered. Then, n_v can reach 10^{-2} and the vacancy has a great influence on the properties of PtCuSi.

Consider the mean nearest neighbor distance *a* in AuCuSi and PtCuSi. At the same *T*, *P* and doping atomic concentration, *a* of defective alloys is less than *a* of perfect alloys. Specifically, The maximum reduction of *a* is 0.24% for AuCuSi and 0.42% for PtCuSi. The reason why n_v reduces *a* is that when there is a vacancy, the bottom of the potential well is shifted closer to the coordinate origin (see Figure 6 and Figure 7), the atomic coordination number decreases, the lattice is no longer tightly bound as before and the pressure easily causes the atoms to be squeezed closer together.

Consider the dependence of the thermal expansion coeficient α_T on *T* and *P*. At the same *P* and doping atomic concentration, α_T increases withn *T*, still at the same *T* and doping atomic concentration, α_T decreases with *P*. This agrees with experiments. For alloys at the same *T* and *P* when c_{Si} increases, α_T decreases. If considering the perfect alloys or the defective alloys alone, although the dependence of α_T on c_{Cu} is less than that of c_{Si} but c_{Cu} plays an important role in making the difference between α_T of perfect alloys and α_T of defective alloys as well as other properties. If the interstitial atom interferes with the vacancy formation, the substitutional atom facilitates the vacancy formation. Substitutional atoms and lattice defects increase the asymmetry of the cohesive energy's graph and that make the anharrmonicity effect of lattice vibrations more evident. Therefore under the same physical conditions, α_T of the perfect alloys is lower than α_T of the defective alloys. α_T is the most "sensitive" quantity for lattice defects. For AuCuSi when $P = 0$, $T = 800$ K, $c_{\mathrm{Cu}} = 4\%$, $c_{\mathrm{Si}} = 1\%$, the conditions are all unfavorable for the formation of vacancies but α_T still increases about 1.13% compared to the ideal case. In the entire investigated scope, α_T of defective AuCuSi increases up to 2.99%. Still for PtCuSi also at $P = 0$, $T = 800$ K, $c_{\mathrm{Cu}} = 4\%$, $c_{\mathrm{Si}} = 1\%$, α_T increases about 1.08%. Especially when *T* and *P* increase up to 2000 K and 80 GPa, α_T of defective PtCuSi maximizes to 7.02% compared to perfect PtCuSi. This is important in engineering when designing physical systems that operate over a wide range of temperatures and pressures.

The dependence of the heat capacity at constant pressure C_P on *T*, *P* and doping atomic concentration for AuCuSi and PtCuSi is the same as α_T. However, at the same doping atomic concentration, The variation of C_P with *T* and *P* is not as strong as α_T. This is consistent with quantum statistical physics theory and experiments when studying solids in high *T* and *P* regions. Under the same physical conditions, C_P of the perfect alloys is lower than C_P of the defective alloys. In the investigated scope, C_P of AuCuSi increases from 0.0019% to 0.26%, still C_P of PtCuSi increases from 0.0004% to 8.56%. The lower the c_{Si}, the higher the *T*, *P* and c_{Cu}, the more obvious the difference and vice versa. Under the same physical conditions, the change of C_P for defective and perfect PtCuSi is correspondingly smaller than the change of C_P for AuCuSi. Alloy PtCuSi can be studied and applied in very high T and P regions and therefore, n_v is very large and the thermodynamic properties of this defective alloy have a strong change.

For AuCuSi at $P = 0$, we obtain the same thermodynamic properties as our previous paper [9]. For AuCuSi at $c_{\text{Cu}} = 0$, we obtain the same thermodynamic properties of AuSi as our previous paper [7]. For AuCuSi at $c_{\text{Cu}} = c_{\text{Si}} = 0$, we obtain the same thermodynamic properties of Au as in [15]. Our calculated results for α_T and C_P of Au and Pt are in good agreement with experiments as shown in tables from Table 2 to Table 4.

Table 2. Dependence of thermal expansion coefficient on temperature for Au at P = 0

T (K)	400	500	600	700	800	1000	1200
α_T (p)-SMM (10^{-5} K^{-1})	1.50	1.55	1.60	1.66	1.72	1.84	1.99
α_T (d)-SMM (10^{-5} K^{-1})						1.85	2.00
α_T -EXPT [17] (10^{-5} K^{-1})	1.45	1.50	1.54	1.59	1.65	1.79	1.95

Table 3. Dependence of heat capacity at constant pressure on temperature for Au at P = 0

T (K)	400	500	600	700	800	1000	1200
C_P (p)-SMM (J/mol.K)	25.562	25.86	26.15	26.48	26.76	27.45	28.25
C_P (d)-SMM (J/mol.K)	25.56	25.86	26.15	26.48	26.76	27.46	28.28
C_P-EXPT [17] (J/mol.K)	25.86	26.27	26.78	27.28	27.82	28.87	29.91

Table 4. Dependence of heat capacity at constant pressure on temperature for Pt at P = 0

T (K)	500	600	700	800	1000	1200
C_P (p)-SMM (J/mol.K)	25.31	25.52	25.69	25.91	26.64	27.72
C_P (d)-SMM (J/mol.K)	25.31	25.52	25.69	25.91	26.64	27.73
C_P -EXPT [18] (J/mol.K)	26.99	27.49	28.03	28.58	29.66	30.79

3. Conclusions

We present the thermodynamic theory for FCC defective ternary substitutional and interstitial alloy ABC derived by the statistical moment method. The obtained thermodynamic quantities depend on temperature, pressure, the concentration of substitutional atoms, the concentration of interstitial atoms, and equilibrium vacancy concentration. Thermodynamic quantities of FCC defective metal A, FCC defective substitutional alloy AB, and FCC defective interstitial alloy AC are specific cases for thermodynamic quantities of FCC defective ternary substitutional and interstitial alloy ABC.

The theoretical results are calculated numerically to alloys AuCuSi, and PtCuSi. The thermodynamic properties of Au, AuSi and AuCuSi calculated in [7, 9, 15] are specific cases obtained in this paper. Our calculated results of thermal expansion coefficient and heat capacities at constant pressure for main metals Au, Pt are in good agreement with experimental data. Our other calculated results for thermodynamic quantities of alloys AuCuSi and PtCuSi at different temperatures, pressure, the concentration of substitutional atoms, and concentration of interstitial atoms orient and predict new experimental data in the future

REFERENCES

[1] G.Li, G.R.Blake and T.T.M.Palstra, 2017. Vacancies in functional materials for clean energy storage and harvesting: the perfect imperfection. *Chemical Society Reviews*, Vol. 46, pp. 1693-1706.

[2] Y.Shi, L.Peng, Y.Ding, Y.Zhao and G.Yu, 2015. Nanostructured conductive polymers for advanced energy storage. *Chemical Society Reviews*, Vol. 44, pp. 6684-6696.

[3] Q.Guo, C.Zhou, Z.Ma, Z.Ren, H.Fan and X.Yang, 2016. Elementary photocatalytic chemistry on TiO_2 surfaces. *Chemical Society Reviews*, Vol. 45, pp. 3701-3730.

[4] R.Schirhagl, K.Chang, M.Loretz and C.L.Degen, 2014. Nitrogen-vacancy centers in diamond: nanoscale sensors for physics and biology. *Annual Review of Physical Chemistry*, Vol. 65, pp. 83-105.

[5] Y.Sun, S.Gao, F. Lei and Y.Xie, 2015. Atomically-thin two-dimentional sheets for understanding active sites in catalysis. *Chemical Society Reviews*, Vol. 44, pp. 623-636.

[6] N.Q.Học, L.H.Viet, N.N.L.Anh and N.B.Ngọc, 2017. The influence of vacancies on thermodynamic properties of BCC interstitial alloy ABC at zero pressure. *HNUE Journal of Science, Natural Sci.*, Vol. 62, No. 2, pp. 27-36.

[7] N.Q.Hoc, P.T.M.Hanh and L.H.Viet, 2016. Thermodynamic property of interstitial alloy AuSi with a vacancy and FCC structure: Dependence on temperature, concentration of interstitial atoms and the concentration of equilibrium vacancies. Proceedings of the 8th International Workshop on Advanced Materials Science and Nanotechnology (IWAMSN-8), 8-12th November, Ha Long city, Vietnam, Publishing House for Science and Technology, p. 293-301.

[8] N.Q.Hoc and L.H.Viet, 2017. Influence of vacancy on thermodynamic properties of interstitial alloy FeSi with BCC structure under pressure. Proceedings of the 10th National Conference on Solid State Physics and Material Science (*SPMS*), Hue City, 19-21, October, pp. 907-910.

[9] N.Q.Hoc, P.T.M.Hanh and L.H.Viet, 2017. Influence of vacancy on thermodynamic properties of interstitial alloy AuCuSi with FCC structure at zero pressure. Proceedings of the Conference "Transactions on Physics and Education" of HPU2, 15 December, Xuan Hoa Town, Vinh Phuc Province. *Journal of Science of Hanoi Pedagogical University No.2*, No. 50, pp.118-129.

[10] N.Q.Hoc, P.T.M.Hanh, D.T.Huong, D.B.Ngoc, T.T.Huyen and L.H.Viet, 2018. Influence of vacancy on thermal expansion coefficient and heat capacity at a

constant pressure of interstitial alloy FeCrSi with BCC structure at zero pressure. *Journal of Military Science and Technology,* No. 54A, pp. 68-77.

[11] L.T.C.Tuyen, N.Q.Hoc, B.D.Tinh, P.T.M.Hanh, T.D.Cuong and L.H.Viet, 2019. Thermal expansion coefficient of BCC defective substitutional alloy AB with interstitial atom C. *Modern Physical Letter B,* Vol. 33, No. 13, Article ID 1950165.

[12] N.T.Hoa, N.Q.Hoc, G.Coman, T.D.Cuong and L.H.Viet, 2019. Thermodynamic property of FCC interstitial alloy with defects. Proceedings of the 8th International Conference on Material Science and Engineering (UGALMAT 2018), 11 - 13 October, 2018, “Dunarea de Jos” University of Galati, Romania, *IOP Conference Series: Materials Science and Engineering,* Vol. 485, Article ID 012018.

[13] N.Q.Hoc, V.D.Lam, P.T.M.Hanh, T.D.Cuong and L.H.Viet, 2018. Heat capacity at a constant pressure of defective FCC substitutional alloy AB with interstitial atom C. Proceedings of the 9th International Workshop on Advanced Materials Science and Nanotechnology (IWAMSN 2018), Ninh Binh province, Vietnam, 7 - 11th November, pp. 49-56.

[14] N. Tang and V.V.Hung, 1989. *Physica Status Solidi (b),* Vol. 149.

[15] V.V.Hung, 2009. *The statistical moment method in studying elastic and thermodynamic properties of crystals*. HNUE Publishing House, Hanoi.

[16] M.N.Mogomedov, 1987. On calculating the Debye temperature and the Gruneisen parameter. *Zhurnal Fizucheskoi Khimii,* Vol. 61, No. 4, pp.1003-1009 (in Russian).

[17] *American Institute of Physics Handbook,* 1963, New York.

[18] W. B. Pearson, 1958. *A Handbook of Lattice Spacings of Metals and Alloys.* Pergamon, New York.